The proangiogenic potential of a novel calcium releasing composite biomaterial: orthotopic *in vivo* evaluation

Hugo Oliveira[1,2], Sylvain Catros[1,2,3], Oscar Castano [4,5,7], Sylvie Rey[1,2], Robin Siadous[1,2], Douglas Clift[4,5], Joan Marti-Munoz[4,5], Marc Batista[4,5], Reine Bareille[1,2], Josep Planell[4,5,7], Elisabeth Engel[4,5,6], Joëlle Amédée[1,2]

[1] University of Bordeaux, Tissue Bioengineering, U1026, F-33076 Bordeaux, France

[2] Inserm, Tissue Bioengineering, U1026, F-33076 Bordeaux, France

[3] CHU Bordeaux, Services d'Odontologie et de Santé Buccale, F-33076 Bordeaux, France

[4] Institute for Bioengineering of Catalonia (IBEC), Barcelona, Spain

[5] CIBER en Bioingeniería, Biomateriales y Nanomedicina, CIBER-BBN, 50018

Zaragoza, Spain

[6] Materials Science and Metallurgical Engineering, Universitat Politècnica de Catalunya, Barcelona, Spain

[7] Materials Science and Physical Chemistry, Universitat de Barcelona, Barcelona, Spain

Corresponding author: Hugo Oliveira.

Address: Inserm U1026 Biotis, Zone Nord, Bât. 4a, 2ème étage,

146 rue Léo Saignat 33076 Bordeaux cedex, France

Telephone: +33 (0)5 57 57 11 90

Email: hugo.de-oliveira@inserm.fr

Abstract

Insufficient angiogenesis remains a major hurdle in current bone tissue engineering strategies. An extensive body of work has focused on the use of angiogenic factors or endothelial progenitor cells. However, these approaches are inherently complex, in terms of regulatory and methodologic implementation, and present a high cost. In this sense, simpler and more cost effective alternatives are awaited. We have recently demonstrate the potential of electrospun poly(lactic acid) (PLA) fiber-based membranes, containing calcium phosphate (CaP) ormoglass particles, to elicit angiogenesis *in vivo*, in a subcutaneous model in mice by fast calcium ion release. Here we have devised an injectable composite, containing CaP glass-ceramic particles dispersed within a HPMC matrix, with the capacity to release calcium in a more sustained fashion combined with the aforementioned fiber-based mats acting as enevelope. We show that by tuning the release of calcium, *in* vivo in a rat bone defect model, we could improve both bone formation and increase angiogenesis. This methodology allows to integrate two fundamental processes for bone tissue regeneration while using a simple, cost effective and safe approach.

Keywords

Angiogenesis, Bone regeneration, Calcium phosphate ormoglasses

1. Introduction

Current bone regeneration approaches still face a wide range of limitations that in combination to the increased incidence of bone pathologies linked to the general population aging profile it continues to pose an important health challenge. Present regeneration approaches are focused

on three main strategies: **1**) autologous bone grafts that, although the gold standard for bone regeneration and the most common approach, implies a two stage time consuming surgical procedure, that requires patients in general good health and is often associated with significant morbidity, post-operative pain, hypersensitivity, infection and paresthesia [1-4]; **2**) allogeneic bone grafts, often associated with immunogenic and infection risks [5]; and **3**) bone substitutes, based on biodegradable polymers and/or synthetic ceramics, increasingly being studied as bone tissue engineering material as they can be established as an off-the-shelf clinical product [6]. This last approach, although with great potential to satisfy clinical need, has shown insufficient vascularization and osteointegration, when in the absence of autologous cells and/or proangiogenic factors [7]. Indeed, attempts to stimulate neovascularization, by the use of recombinant protein, angiogenic growth factors gene transfer or endothelial cells have been proposed, however often associated with problems regarding the delivery and duration of exposure to the growth factors and with the survival of endothelial cells [7]. Additionally, due to inherent risks, the use of growth factors and autologous cells presents additional regulatory hurdles, particularly relevant in some cases of bone repair post cancer resection [8]. Hence, in order to fulfill the promise of bone tissue engineering the problematic of neovascularization, inside the implanted constructs, has to be solved in order to reach the bedside. This drawback is particularly relevant in large bone defects, where the amount of oxygen required for cell survival is limited to a diffusion distance between 150-200 μm from the supplying blood vessels [9]. Nonetheless, in view of a broad clinical application, the establishment of off-the-shelf strategies may prove beneficial and reduce regulatory issues. As such, the use of synthetic polymeric matrices, that can be readily engineered and custom designed, may show the future for new bone therapeutic approaches.

We have recently demonstrated the potential of electrospun poly(lactic acid) (PLA) fiber-based membranes, containing calcium phosphate ormoglass (CaP) particles, to elicit angiogenesis *in*

vivo, in a subcutaneous model in mice [10]. These CaP particles with capacity to release bioactive calcium ions, in a controlled fashion, are an alternative cost effective approach in order to achieve ready-to-use bone substitutes. Based on the observation that sudden increased local concentration of calcium (Ca^{2+}) ions could induce the migration, maturation and organization of endothelial progenitors [11], we could demonstrate *in vivo* that these materials could elicit the local expression of angiogenic factors, associated to a chemotactic effect on macrophages, and sustain angiogenesis into the biomaterial [10].

On the other hand, calcium phosphate glass ceramic are a very promising alternative for a more progressive ion release rate as crystalline phases use to degrade slower than glassy ones [Navarro et al. Biomaterials. 2004 Aug;25(18):4233-41]. Our hypothesis is based on the slower and longer healing of the inner part of the bone tissue and thus the required Ca^{2+} stimulation should be slower and more sustained.

Here we evaluated the use of a sol-gel prepared CaP glass-ceramic in an orthotopic model, in a condylar defect in rat, to sustain both bone repair and angiogenesis. We tested different calcination temperatures, in order to tune Ca^{2+} release profiles, formulated them as an injectable composite and associated it with a PLA/ormoglass contention membrane.

2. Materials and Methods

2.1. Reagents

Unless mentioned otherwise, all reagents were obtained from Sigma-Aldrich and were of analytical grade.

2.2. Scaffolds fabrication and characterization

Sol-gel alkoxide precursor solutions were prepared by refluxing them in proper solvents, except Ti tetraisopropoxide was commercially obtained (ALFA AESAR, 97%) and diluted in absolute ethanol. Ca and Na precursor solutions were prepared by refluxing metallic Ca and Na in 2-methoxyethanol. P precursor solution was obtained by refluxing P_2O_5 in absolute ethanol.

2.2.1. Electrospun PLA mats with embedded NP

CaP ormoglass NPs were prepared by a partial hydrolyzed alkoxides sol-gel method with a composition of 44.5:44.5:6:5 $CaO:P_2O_5:Na_2O:TiO_2$ molar ratio, following a previous report [12]. After mixing Ca, Na an Ti precursor solutions in the proper molar ratio in inert atmosphere, a catalyst with a composition related to Ti ($Ti:H_2O:NH_3$:EtOH 1:60:0.3:12) was added at 4ºC at 2 ml/h using an infusion pump. Afterwards, P precursor was similarly added at 4ºC and 1 ml/h flow. The mix turned from dark brown to clear orange and it was subsequently hold at 70ºC during 4 days for aging and allow the formation of NPs. They were finally collected and washed with absolute ethanol by centrifugation and dried at 90ºC in the oven.

Nanofiber mats were prepared as previously described [10]. Briefly, PLA nanofibers loaded with 20% (w/w) of CaP ormoglasses (labelled as PLA CaP) were prepared by the ultrasonic dispersion of the nanoparticles in a 4% (w/v) PLA (Purasorb PLDL 7038, inherent viscosity midpoint 3.8 dl/g, molecular mass ≈ 850,000 Da) solution. Slurries were electrospun at 8.000V, 150 mm distance tip-collector and at 1200 rpm rotary collector speed.

2.3. Nanostructured G8 glass-ceramic injectable gels fabrication

To prepare the glass-ceramic material Ca, Na and Ti precursor solutions were mixed in inert atmosphere in the proper molar ratio, similarly to previous process. P precursor solution was then added at 4ºC and a rate of 2.5 mL/h using an infusion pump. Then, an acid aqueous catalyst with a Ti molar relation of Ti:20 H_2O:0.1 HCl:5 isopropyl alcohol was added at a rate of 1 mL/h and 4ºC. The mix was sealed and left to rest for 24 hours at room temperature and then heated

at 80ºC for 3 days. The resulting liquid part was poured and eliminated, and the solid gel heated at 120ºC for 12 hours at air. The resulting powder was grounded and hold to a thermal treatment at 500, 540, 570 or 610ºC (labelled as CaP 500, CaP 540, CaP 570 and CaP 610) for 5 hours. The final powder was milled and sieved to obtain sintered nanoparticles agglomerates smaller than 40 μm.

(Hydroxypropyl)methyl cellulose (HPMC, Mn 90 000 Da, Sigma) was dissolved in Phosphate buffer saline (PBS) to a final concentration of 2% (w/v) and sterilized by autoclaving. In order to formulate the composite gel, 40% (w/v) of CaP particles were dispersed in the HPMC gel.

Both constructs, produced as stated in sections 2.2 and 2.3, were then combined for the in vivo assays.

2.4. Calcium release, FE-SEM characterization and chemical composition.

Calcium release from the glass-ceramics powders was measured using an ion selective electrode. 15 mg of glass or glass-ceramic powder samples were bathed in 750 μL of 0.01 M HEPES buffer solution and incubated at 37°C. Bathing fluid was removed periodically (every 3-4 days) for a period of 36 days and pH and calcium ions were measured in the removed solution. pH was measured with a Crison GLP22 (Crison, SPAIN), while electrical potential of the solution was measured with a combined calcium selective polymer-membrane electrode (Metrohm AG, Herisau Switzerland). Electrical potential values read from the solution were compared to measurements from calibration solutions to determine calcium concentrations of the samples.

Micro- and Nano-morphology was measured using an Ultra-High Resolution Field Emission Scanning Electron Microscopy (Nova Nano SEM-230; FEI Co., Netherlands), operating at 5.00 Kv and coating the samples with an ultra-thin layer of carbon to make them conductive.

Material's composition was assessed using an Energy Dispersive X-ray Spectrometer (EDS, Quanta 200 XTE 325/D8395; FEI Co.). Materials were also coated with a thin layer of carbon before analysis.

2.5. Glass transition temperature and simultaneous thermogravimetric (TGA) and differential thermal analysis (DTA).

Glass transition temperature was measured on a Q20 differential scanning calorimeter (TA instruments, USA). A heating rate of 10°C/min to 600°C was used. Simultaneous thermogravimetric and differential thermal analysis of the sol-gel sample was executed on a Netzsch STA 409 C/CD instrument (NETZSCH-Gerätebau GmbH, Germany). A heating rate of 10°C/min to 900°C was used.

2.6. X-ray diffraction

XRD was measured on a PANalytical X'pert PRO MPD Alpha1 powder diffractometer. Patterns were collected from $2\theta = 4.2$ to 80° with a step size of 0.017° and a measuring time of 50 seconds per step.

2.7. Organic Elemental Analysis

Powder glass-ceramic samples were analyzed after heat treatment to determine residual carbon using a Carlo Erba Instruments Thermo Flash 2000 (Carlo Erba, Milan, Italy). This method is based on a Gas chromatography after total decomposition and oxidation of the sample at high temperature (~1800ºC). For that purpose, 100mg samples were used..

2.8. Cell culture

Human progenitor-derived endothelial cells (PDECs) were obtained as previously described [13]. Briefly, human umbilical cord blood from healthy donors (between 20 and 35 years) were diluted with one part of PBS, 2% (v/v) fetal calf serum (FCS) and 2 mM ethylene diamine

tetraacetic acid (EDTA), and applied to a density gradient centrifugation in Histopaque® solution (1.077 $g.mL^{-1}$). Mononuclear cells were recovered from the buffy coat, washed several times with PBS and cultured in endothelial cell growth medium-2 (EGM-2; Lonza-Verviers, France) containing all kit supplements and 5% (v/v) FCS (GIBCO Life Technologies, Karlsruhe, Germany), on collagen-coated 12-well plates (collagen type I from rat tail, BD Biosciences) and at $5x10^7$ cells per cm^2. At day 4, non-adherent cells were removed and medium was refreshed every other day. After 2–3 weeks, cobblestone-like morphology colonies were harvested, using 0.25% (w/v) trypsin–EDTA (GIBCO) and subcultured in fresh collagen-coated dishes. Cells were expanded over several passages, using standard cell culture procedures.

2.9. *In vitro* evaluation

Twenty-four hours prior, PDECs were seeded on 24 well plates at $20x10^3/cm^2$ and cultured using 500 µL of endothelial cell growth medium-2 (EGM-2; Lonza-Verviers, France). Then, 50 µL of HPMC gels, containing 40% (w/v) of CaP particles sintered at 540 or 570 degrees, were placed inside a 0.4 µm pore transwell (Corning, EMEA, France) and set in contact with the cell culture medium. At designated time points cells were processed for viability assay or cells culture medium was assessed for VEGF quantification.

2.10. Cell viability assessment

Cytotoxicity assessment on human PDECs was performed according to the standard ISO/EN 10993, part 5, guidelines and using the neutral red assay. Briefly, 24 hrs post exposure to the HPMC gels, through the transwell inserts, and the colorimetric neutral red assay was performed according to established protocols [14].

2.11. VEGF secretion evaluation

In order to assess the capacity of the different materials to induce the secretion of vascular endothelial growth factor (VEGF), the cell culture medium of PDECs cultured on the different materials for 4 days was recovered, snap frozen and kept at -80ºC until further use. Secreted VEGF was evaluated by ELISA assay using a commercial kit (human VEGF ELISA, #DVE00, R&D Systems, USA) following the manufacturer's instructions.

2.12. Animal procedures

As an initial model to assess the capacity of the developed materials to sustain bone repair we implanted them in a bone defect model in rats, condylar defect. All the procedures for rat handling were based on the principles of Laboratory Animal Care formulated by the National Society for Medical Research and approved by the Animal Care and Experiment Committee of University of Bordeaux, Bordeaux, France. Experiments were carried out in accredited animal facilities following European recommendations for laboratory animal care (directive 86/609 CEE of 24/11/86).

Medial holes, 4 mm diameter and 6 mm depth were created in both left and right femoral condyles of Wistar rats weighing 200-250 g (Charles River Laboratories, France). Bone pieces were removed from the defect, and the holes were rinsed with physiological solution (NaCl 0.9 % (w/v)) before injecting the Hydroxypropyl Methylcellulose (HPMC) gel, containing or not 40% (w/v) of calcium phosphate particles, sintered at two different temperatures (*i.e.* 540 or 570 ºC). The PLA membrane, containing or not 20% (w/w) NPs (as previously described in Oliveira et al. Acta Biomaterialia 29(), 435-445) was used to constrain the gel inside the defect and to start vascularization on the defect side. At 3 and 6 weeks animals were sacrificed by CO_2 inhalation and femoral bones were recovered for histologic, immunohistochemistry and μCT evaluation. Six independent materials were implanted per tested material and per time point.

2.13. X-ray microtomography and analysis

Micro-CT was performed on Explore Locus SP X-ray m-CT devices (General Electric, Milwaukee, WI) *ex vivo* with a source voltage of 80 kV and a current of 60 mA to obtain a 15 mm resolution from 900 X-ray radiographs with an exposure time of 3000 ms. After scanning, cross-sectional slices were reconstructed and three-dimensional analysis were performed using eXplore MicroView software (General Electric Healthcare, Milwaukee, WI). Reconstruction of the region of interest was performed after correction of the center of rotation and calibration of mineral density. Each scan was reconstructed using the same calibration system to distinguish bone and air. Bone volume (BV) per total volume (TV) was determined for each sample.

2.14. Histological analysis

The femoral and tibial bones were recovered, fixed with 4% (w/v) paraformaldehyde for 48 hrs at 4°C and then demineralized (Microdec, Diapath, France), dehydrated and embedded in paraffin. Eight microns sections were cut and stained with Masson's Trichrome for osteoid staining, using standard protocols, and observed under a photomicroscope (Nikon eclipse 80i, The Netherlands).

2.15. Immunohistochemistry analysis

Immunohistochemistry for CD31 was performed as follows. Eight-micron paraffin sections were cut, deparafinized, rehydrated using ethanol gradients and placed in PBS. Antigen recovery was performed using a proteinase K (Roche, France) digestion procedure and then endogenous peroxidase was quenched using 3% (v/v) hydrogen peroxide for 5 min at room temperature (RT). Tissues were blocked with 2% horse serum, in PBS, for 30 min at RT. Primary antibody against CD31 (NB100-2284, Novus Biologicals, Bio-Techne, France) was used at 1:100 in 2% (w/v) BSA in PBS, and incubated overnight at 4°C. After two washes with PBS, the anti rabbit Impress kit (VectorLabs, USA) was used according to the manufacturer's

instructions. Specific staining was obtained using the 3,3'-diaminobenzidine staining solution (VectorLabs, USA). Counterstaining was performed using Mayer's haematoxylin. Samples were then mounted using Pertex medium (Sigma). Sample imaging was performed using a microscope (Nikon Eclipse 80i) equipped with a digital camera (Nikon Dxm 1200C). Sample analysis was performed at three different sample positions and a total of six animal samples were assessed per time point and condition. For vessel quantification the total number of micro vessels was determined and normalized to the area of the defect.

2.16. Statistical analysis

Using the Graphpad Prism 5.0 software, a D'Agostino and Pearson omnibus normality test was used in order to test if data obeyed to a Gaussian distribution. Statistically significant differences between several groups were analyzed by the non-parametric Kruskal-Wallis test, followed by a Dunns post-test. The non-parametric Mann-Whitney test was used to compare two groups. A p value lower than 0.05 was considered to be statistically significant.

3. Results

3.1. Biomaterial synthesis and characterization

Differential thermal analysis (DTA) is a powerful tool when considering sol-gel glasses analysis, due to the ability to evaluate the chemical changes that occur during the calcination steps. **Figure 1A** displays the DTA plot for the sol-gel material, and in this representation, exothermic reactions correspond to a downward peak on the y-axis. The gravimetric portion of this plot is characterized by a series of downward steps, as materials are burned away during calcination. These downward steps correspond with peaks in the thermometric plot, signifying a chemical change in the sample. The major events in the sol-gel material include a small mass loss and exothermic peak at around 130°C, which corresponds to the loss of residual water from

the material, and then two endothermic peaks at about 250 and 320°C as the organic residues are eliminated. Indeed, and as observed in **Table 1,** residual carbon content was below 0.1%, consistent with the DTA results. Additionally, glass transition temperature (Tg) was 480ºC in both cases and composition, measured by energy dispersive X-ray spectroscopy (EDS), was as expected (**Table 1**). In order to analyze the formation of the crystalline phase after the calcination of the sol-gel material, an X-ray powder diffraction (XRD) evaluation was performed. **Figure 1B** shows how the final amount of crystallization within the material is closely related to the temperature of calcination. Here, all sol-gel samples are compared at the 4 different temperatures treated. Corresponding to the step-wise increase of calcination temperature, each subsequent material exhibits an increase in crystallinity. The sample calcined at 500 ºC had a completely amorphous behavior, and presented a dark grey color associated to a high carbon content. As such, this sample formulation was discarded from further studies.

The one calcined at 540°C still contains a large amorphous phase, while the powder calcined at 610°C is completely crystalline. Compounds visible in the sol-gel glass ceramic samples include pyrophosphates, both α (α-$Ca_2P_2O_7$, JCPDS 9-345) and β (β-$Ca_2P_2O_7$, JCPDS 9-346), as well as a calcium metaphosphate (δ-$Ca(PO_3)_2$, JCPDS 9-363) and a singular sodium-titanium phosphate $NaTi_2(PO_4)_3$ (JCPDS 84-2008) (**Figure 1B**).

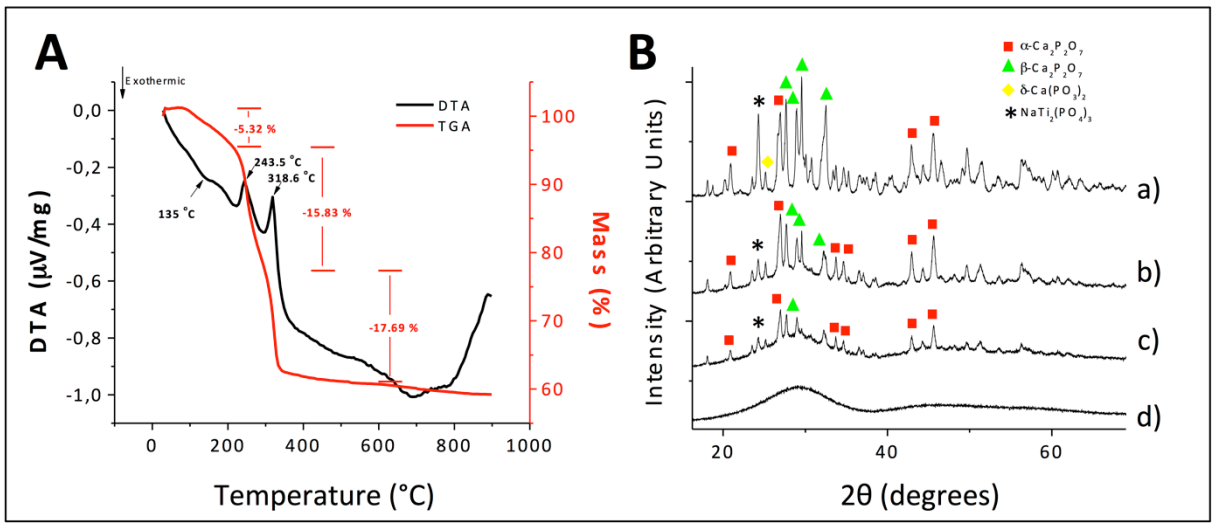

Figure 1- A) Differential thermal analysis (DTA) plot of the sol-gel material. DTA is represented by the solid line with the left axis, while the mass change trace is displayed by a dotted line and corresponds to the right axis. **B)** X-ray powder diffraction (XRD) and phase composition comparison of the sol-gel materials calcined at different temperatures (°C) a) 610, b) 570, c) 540 and d) 500 ºC.

Figure 2A displays the calcium ion release results for the material, in which total ion release is summed over time. Glass-ceramic particles demonstrated a linear release rate, over the entire time frame investigated. Additionally, the plot shows that with increased sample calcination temperature there is a decrease in the solubility of the ceramic, due to the increased crystallinity of the final product. Respectively, the three sol-gel samples CaP540, CaP570 and CaP610 exhibited linear release rates of 0.065, 0.054 and 0.029 mM/day.

As observed in **Figure 2B,** pH remained very closed to physiological one in the glass-ceramic environment, for the 3 tested CaPs. Nonetheless, due to the slow release kinetics of CaP 610 sample, we focused on the CaP540 and CaP570 bioglass formulations in the following studies.

Figures 2A and 2B, show the micrography of both CaP540 and CaP570 showing a nanoscaled crystal particle sizes connected by sintering.

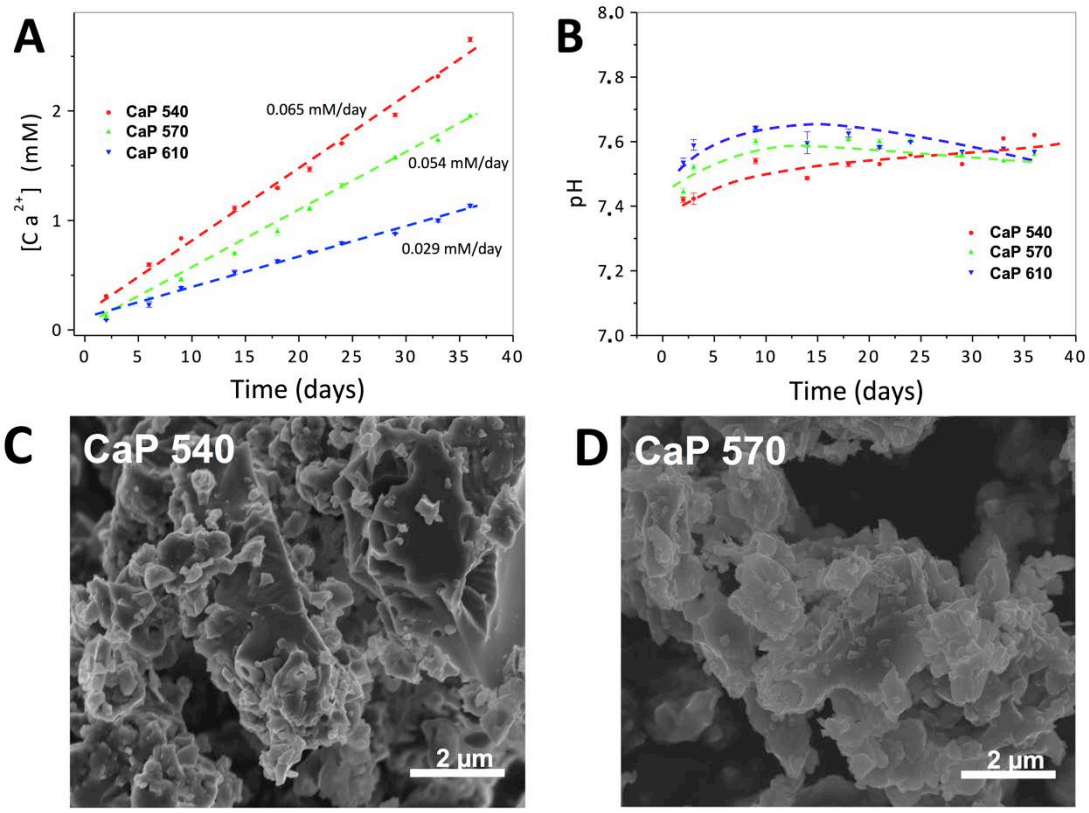

Figure 2- A) Ca^{2+} release and B) pH evaluation from samples calcined at 3 different temperatures and the G5 standard previously reported. **C**) and **D**) are representative micrographies by FE-SEM of nanostructured agglomerates resulting from the glass-ceramic fabrication.

Table 1- Glass transition temperature (Tg), Carbon final content, and oxide based composition of the glass ceramic calcined at 540 and 570ºC (average±SD).

	Tg	Carbon Content (at%)	CaO	P_2O_5	Na_2O	TiO_2
G8-540	480ºC	0.097 ± 0.006	45.3±2.9	44.1±2.4	3.3±1.6	7.2±1.8
G8-570		0.080 ± 0.008	45.6±1.2	42.9±1	3.0±0.5	7.7±0.4

3.2. *In vitro* evaluation

In view of the application of these matrices to bone tissue regeneration and to support angiogenesis we initially tested the influence of the composite biomaterial over human PDECs cell viability. As observed in **figure 3A**, no significant differences could be observed for both CaP formulations, in relation to the control. Additionally, and as means to assess the impact of the composite formulation over the expression of VEGF we performed an ELISA assay to determine the VEGF secretion by PDECs after 4 days of exposure, using a transwell system. As observed in **figure 3B** a significant increase of VEGF secretion was observed for the 540 ºC CaP composite formulation, in relation with the control.

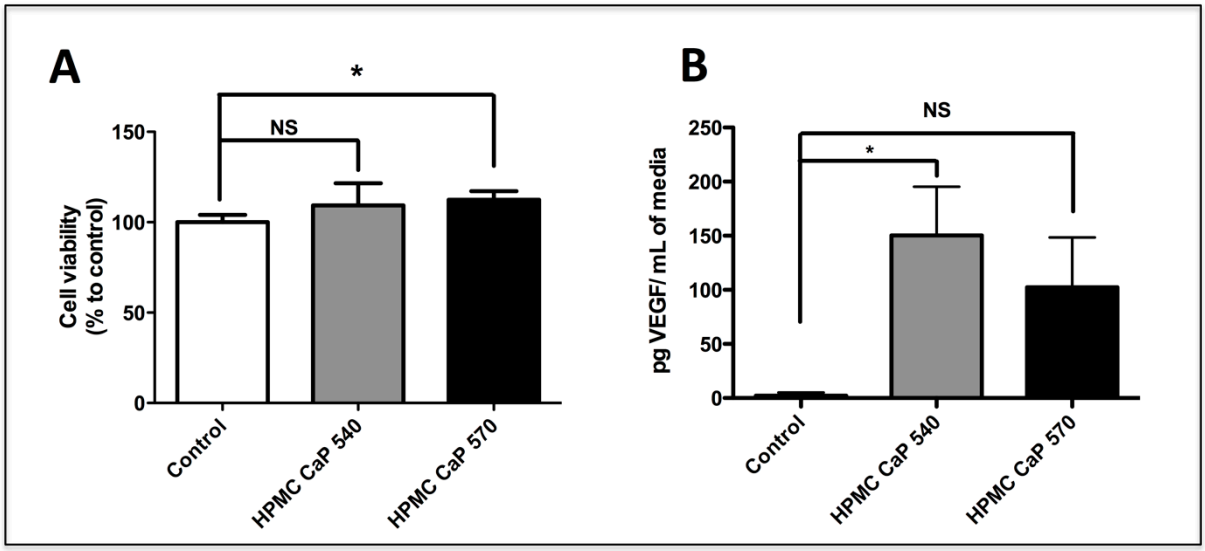

Figure 3- A) Percent cell viability, as measured by the neutral red assay, of human progenitor-derived endothelial cells (PDECs) exposed for 24 hr to (Hydroxypropyl) methyl cellulose (HPMC) gels containing 40% (w/v) of calcium phosphate particles (CaP), sintered at two different temperatures (*i.e.* 540 or 570 ºC) and normalized in relation to the control (Average±SD, n=8, * and NS denotes $p<0.05$ or non significant, respectively). **B**) Quantification of vascular endothelial growth factor (VEGF) expression by PDECs cultured with exposure, during 4 days, to HPMC gels containing 40% (w/v) of CaP, sintered at 540 or 570 ºC (n=4, average±SD; * and NS denotes $p<0.05$ or non significant, respectively).

3.3. *In vivo* evaluation

In view of determining the capacity of the developed composites to sustain bone repair we focused on a bone defect model in the rat condyle. For this purpose, the two developed composite injectable hydrogels, based on sintered CaP at 540 or 570 ºC, were placed in the defect and covered with an electropsun PLA membrane (containing or not 20% (w/w) of CaP particles) previously reported [10]. Bone regeneration was evaluated at 3 and 6 weeks post-implantation using micro CT based 3D reconstruction and histologic evaluation. As observed in **figure 4A** micro CT imaging shows improved calcified tissue formation for the composite formulations containing CaP materials, in relation to HPMC and PLA alone, and at both time points evaluated. These results are confirmed by micro CT quantification of the mineral volume/total volume ratio (BV/TV) for the explanted femurs (**Figure 4B**). A significant improvement on BV/TV was observed for the HPMC 540, at 3 weeks, in relation with HPMC PLA alone. Also, at 6 weeks post implantation both formulations containing CaP particles (*i.e.* HPMC 540 and 570 with PLA membrane 20% Nps) showed significant improved BV/TV, when compared with HPMC PLA alone.

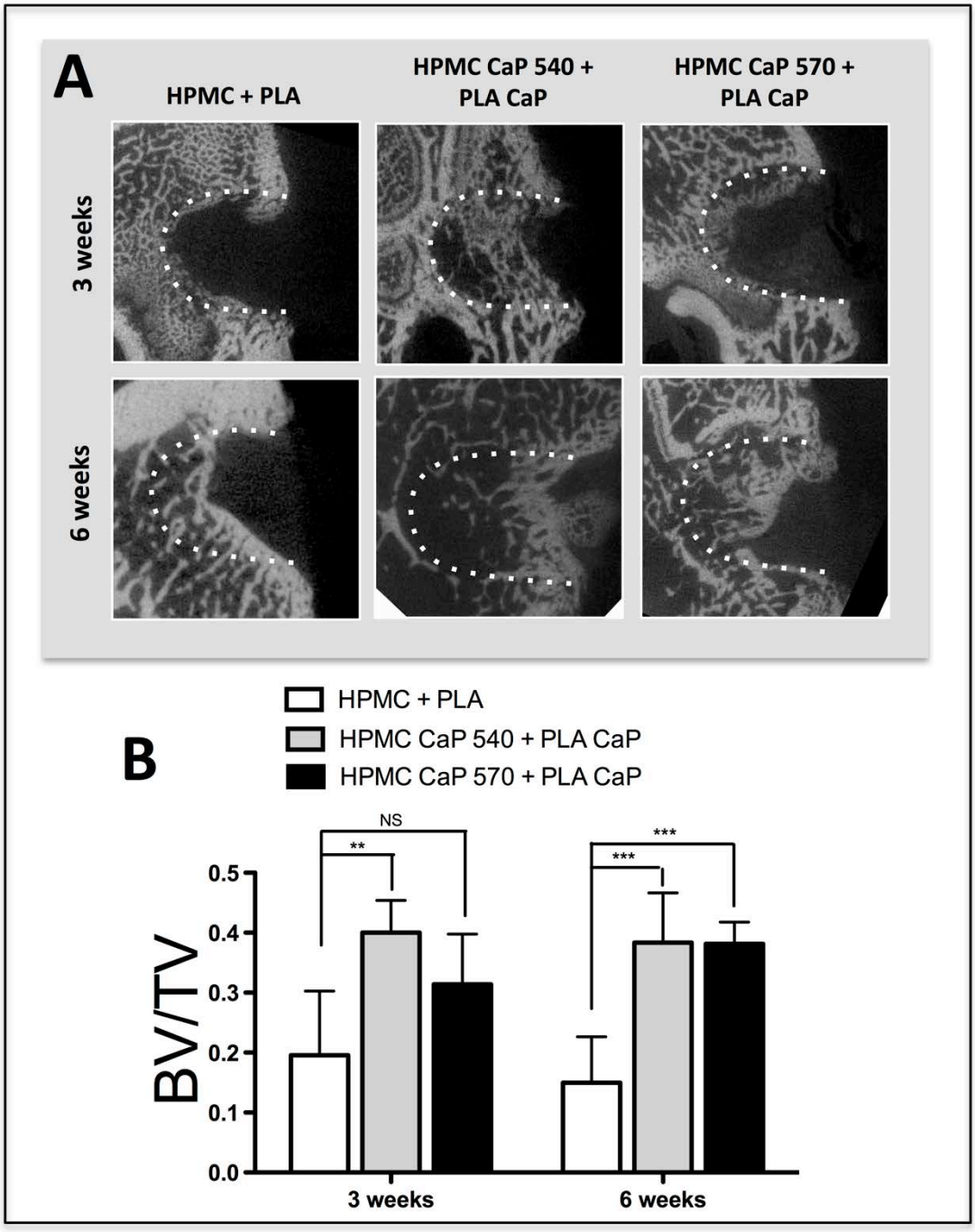

Figure 4- A) Micro-CT representative evaluation of bone formation inside the condylar bone defects when filled with (Hydroxypropyl) methyl cellulose (HPMC) gels containing 40% (w/v) of calcium phosphate particles (CaP), sintered at two different temperatures (i.e. 540 or 570 ºC), and covered with PLA, alone, or containing 20% CaP particles, at 3 and 6 weeks post implantation. **B**) Quantitative assessment of Bone volume/total volume (BV/TV), by μ-CT evaluation, inside the condylar bone defects when filled with HPMC gels containing 40% (w/v)

of CaP particles, sintered at 540 or 570 ºC, and covered with PLA, alone, or containing 20% CaP particles, at 3 and 6 weeks post implantation. (Average±SD, n=6, **, *** and NS denote $p<0.01$, $p<0.001$ and non significant, respectively).

Micro-CT evaluation was then complemented using histologic evaluation. As observed in **Figure 5**, significant osteoid tissue formation could be observed in the case of the formulations containing CaP particles, at both 3 and 6 weeks, and consistent with the results obtained from micro-CT analysis. Also, one can observe that for the two formulations containing CaP particles an increased formation of osteoid tissue (red staining inside the defect) was formed, associated with the deposition of a collagenous matrix (green staining inside the defect, when compared with HMPC and PLA alone (**Figure 5**).

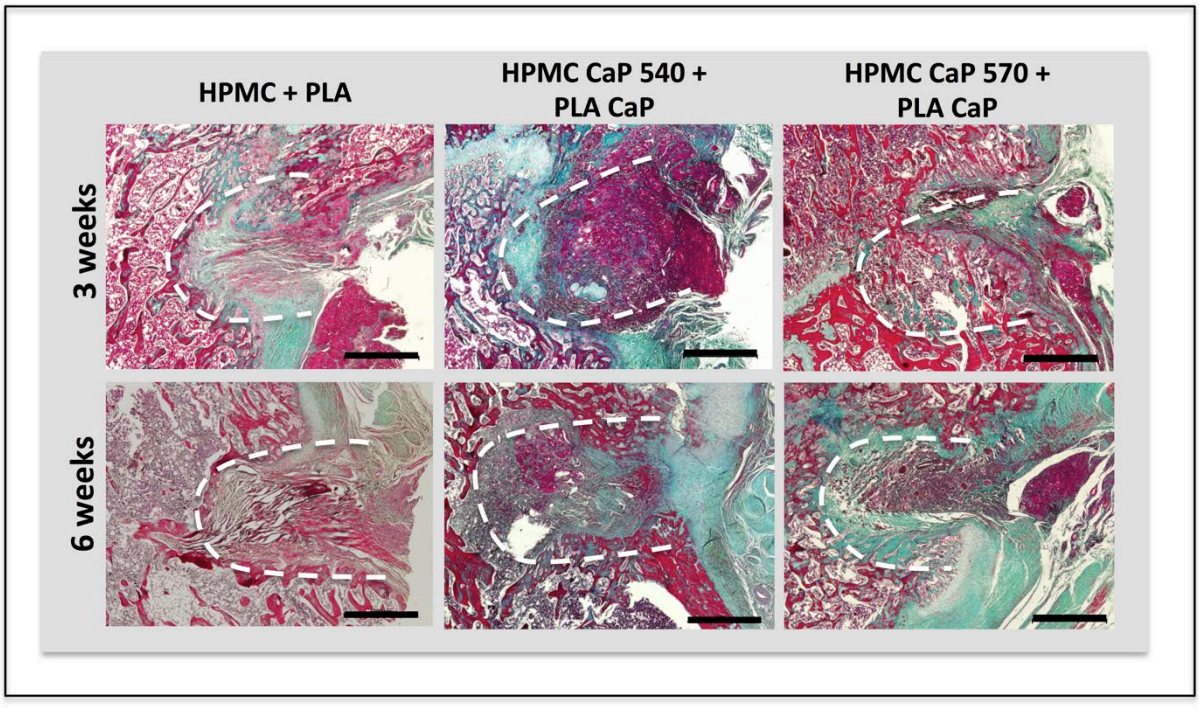

Figure 5- Masson's Trichrome staining of histological sections of the condylar bone defects when filled with (Hydroxypropyl) methyl cellulose (HPMC) gels containing 40% (w/v) of calcium phosphate particles (CaP), sintered at two different temperatures (i.e. 540 or 570 ºC),

and covered with PLA, alone, or containing 20% CaP particles, at 3 and 6 weeks post implantation (scale=1000μm).

In view of evaluating the impact of the different formulations, containing CaP particles sintered at two distinct temperatures (*i.e*. 540 and 570 ºC), on the formation of angiogenesis, we performed an immunohistochemistry for CD31 at 3 and 6 weeks post implantation in a rat condylar defect model. As observed in **Figure 6**, CD31 immunostaining revealed the existence of vessels inside the defect at both 3 and 6 weeks post implantation. The vessel distribution was homogeneous throughout the defect, being visible both at the center and at the periphery, inside the defect.

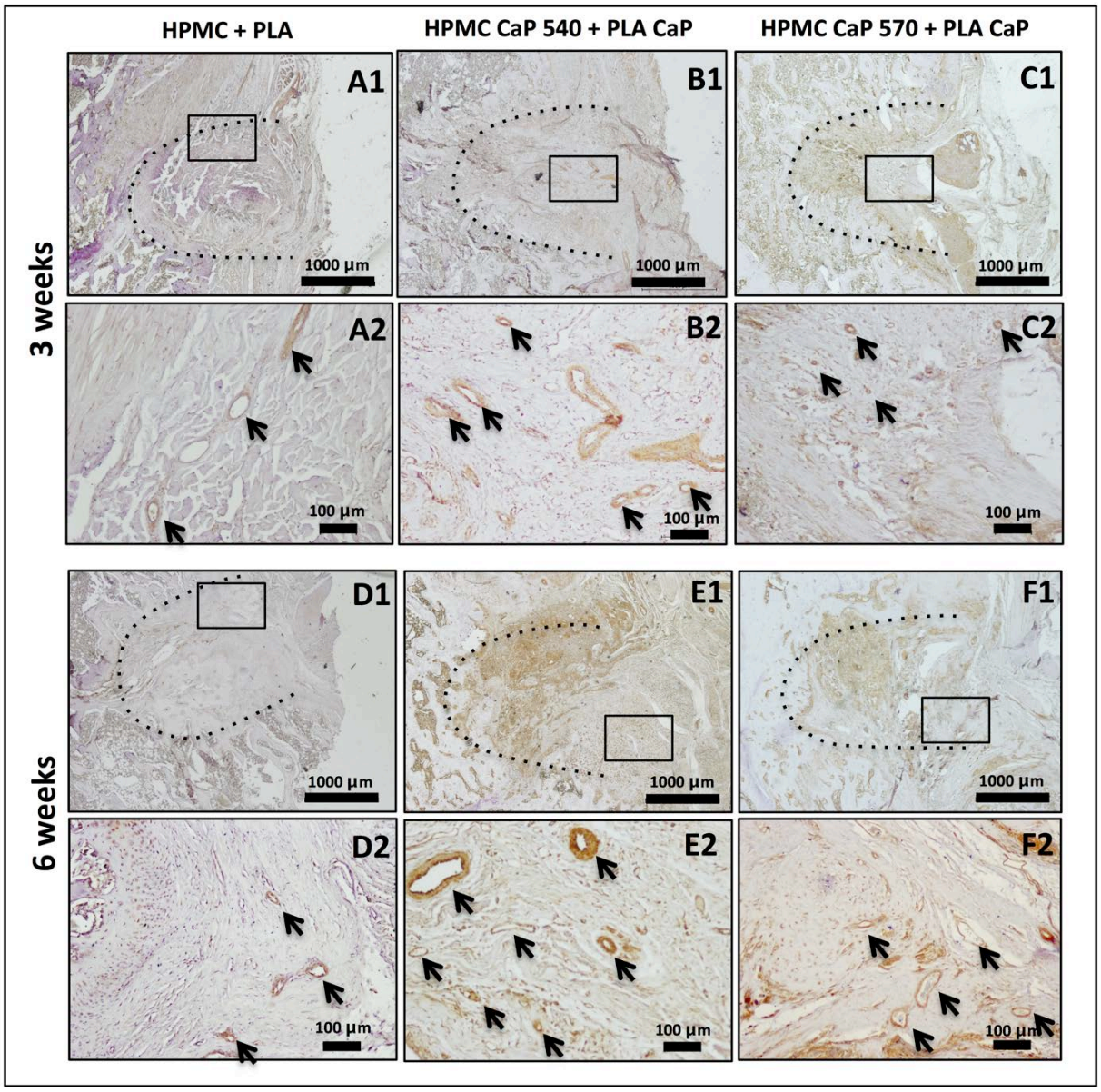

Figure 6- CD31 immunohistochemistry of histological sections of the condylar bone defects when filled with HPMC and covered with PLA alone (**A1**, **A2** and **D1**, **D2**), or containing CaP particles sintered at 540 (**B1**, **B2** and **E1**, **E2**) or 570 ºC (**C1**, **C2** and **F1**, **F2**) and covered with PLA containing 20% CaP particles, at 3 (**A-C**) and 6 (**D-F**) weeks post implantation (scale=1000µm for **A1-F1** or scale=100µm for A2-F2). Blood vessels identified by arrows.

As means to quantify the influence of both the presence of CaP particles within the composite material and of the CaP sintering temperature on angiogenesis we performed vessel

quantification inside the defect. As observed in **Figure 7**, and although no significant differences could be observed at 3 weeks, at 6 weeks post implantation a significant increase for vessel density could be observed for the defects implanted with HPMC containing CaP particles sintered at 540ºC and covered with PLA membranes, containing CaP, in relation to HPMC and PLA alone.

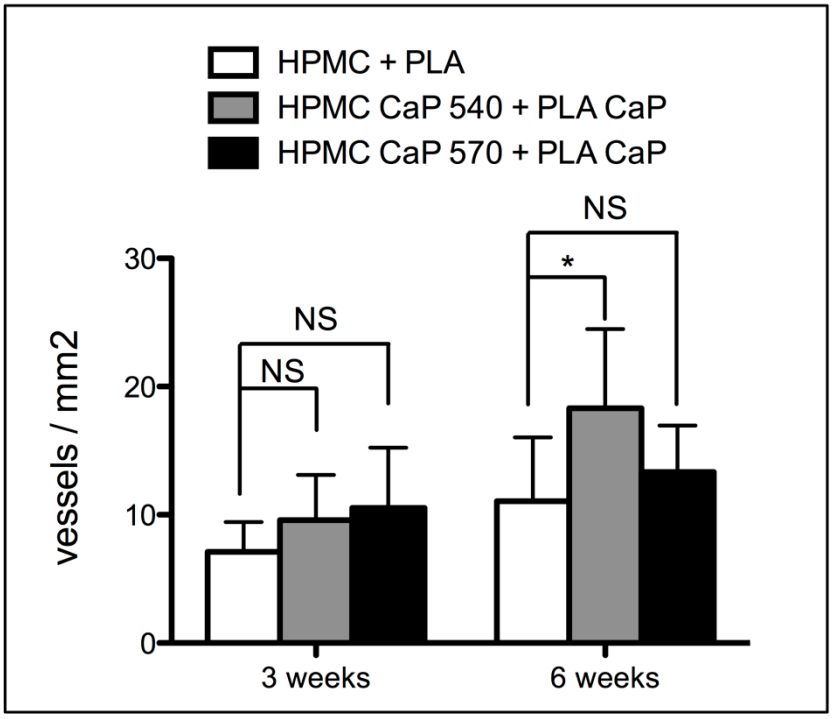

Figure 7 – Quantification of vessel density inside the condylar bone defects when filled with HPMC and covered with PLA alone, or containing CaP particles sintered at 540 or 570 ºC and covered with PLA containing 20% CaP particles, at 3 and 6 weeks post implantation (scale=20µm; n=6, average±SD; * and NS denotes $p<0.05$ and non significant, respectively).

4. Discussion

Autologous bone grafts are still the gold standard when considering the regeneration of bone defects. Nonetheless, they are associated with several drawbacks, including limited graft availability, increased risk of infection and significant morbidity at the donor site [15]. In this sense bone tissue engineering approaches have been proposed as promising alternatives, but in spite of tremendous effort and important advances achieved in the last two decades they have not yet fulfilled their promise [16]. One of the major problematic associated with the efficient translation of bone tissue engineering is the inefficient vascularization of both the implanted constructs and the defect site [6]. In this regard, growing interest has been focused on the development of bioactive biomaterials that can modulate the angiogenesis process, during bone tissue regeneration. Recently, we have shown the potential of electrospun poly(lactic acid) (PLA) fiber-based membranes, containing calcium phosphate ormoglass (CaP) particles, to elicit angiogenesis *in vivo*, in a subcutaneous model in mice [10]. In order to apply this principle to a bone regeneration scenario, here we developed a two component biomaterial approach: 1) a contention membrane of electrospun PLA, containing 20% (w/w) of CaP particles, that was previously optimized [10]; and 2) an injectable gel composed of a new generation of CaP ormoglasses, dispersed at 40% (w/v) in a HPMC gel.

HPMC is a derivate polymer of cellulose that has shown to exhibit suitable biological characteristics and that has already been used for the formulation of injectable biomaterial matrices, containing calcium phosphate ceramics [17-19].

Our first approach was to optimize the conditions of CaP particle production, focusing on their ration of glass/ceramic character, in order to tune their degradation rate and obtain a sustained calcium release profile. As expected, a significant mass loss was observed during the first step

of calcination, up to 350ºC, where the material lost nearly 40% in terms of mass. These results were in agreement with previous reports of sol-gel synthesis of phosphate glasses [20, 21], where at 350ºC the vast majority of the water and extraneous organic material can be eliminated, as shown in **Table 1**.

The use of different calcination temperatures, over the Tg (**Table 1**), shows the appearance of different crystal phases (**Figure 1B**), such as pyrophosphates and the polymorph γ of the tricalcium phosphate. These compounds, as well as the notable absence of calcium-phosphates, have shown to be characteristic of phosphate-based sol-gel and melted glasses [22]. Additionally, the presence of a $NaTi_2(PO4)_3$ peak shows that in spite of the small quantity used, an efficient inclusion of both titanium and sodium, into the crystalline network, was achieved. Also, and although the ratios of these compounds remain similar throughout the heating process, higher processing temperature show to favor the β-calcium pyrophosphate phase. As previously mentioned, the aim was to achieve a blend of both glassy and crystalline CaP ormoglass, as such and due to the high crystallinity of the formulation calcinated at 610ºC, this last was discarded from further studies.

One of the limitations regarding glassy materials resides on their fast degradation, after immersion in fluid, and therefore accelerated release of ions in the first several days, before flattening out to a relatively slow release rate [23]. Conversely, we show that by introducing a nanocrystalline phase we could achieve a constant calcium release rate. This approach allows to tune the release profiles, while maintaining the advantageous zero-order release. Additionally, and in contrast to glassy calcium phosphates materials that usually exhibit a dramatic and immediate pH drop, due to the burst release mechanism [23], our approach shows little pH variation, over the entire time course. This presents an added value for these materials as significant acidifications has shown to induce osteoblast cell death and pro-inflammatory cytokine release by osteoblastic cells [24].

Nonetheless, the thermic process used, necessary to eliminate organics and nucleate the crystal nanophases, shows particle sintering due to the high atomic diffusion. Alternative processes can be used to avoid this issue such as the modification of the thermodynamic stability by altering some experimental conditions or using methods such as spray pyrolysis to avoid the physical contact among particles during the phase's growth.

Following the establishment of two ormoglass formulations, calcined at 540 and 570ºC, and based on previous reports [18, 19], we formulated them at 40% (w/v) in a 2% (w/v) HPMC gel. *In vitro* tests confirm their lack of toxicity for PDECs, under the test conditions, and show a dependence of the calcination temperature on their capacity to elicit VEGF secretion. The HPMC gels containing 40% (w/v) of CaP, sintered at 540 showed the better performance in terms of VEGF secretion. This correlates well with our previous studies were it was demonstrated that Ca^{2+} release from ormoglass particles, in the range of 0.6 - 1 mM, induced expression of VEGF gene and protein secretion [10, 25].

Then, focusing on the application of these composites for bone repair we evaluated their capacity to sustain bone repair in a condylar defect model in rat. Significant improvement in terms of BV/TV was observed for the 540 formulation, at 3 weeks, and for both 540 and 570, at 6 weeks, in relation to the vehicle alone. These results are in line with the Ca^{2+} release kinetics of both the 540 and 570 formulations, where a faster Ca^{2+} release (*i.e*. 540) shows to favor a faster bone repair, evident by micro CT analysis and by the formation of osteoid tissue. Previous studies have indeed shown that elevated Ca^{2+} levels could promote the recruitment of bone marrow progenitor cells *in vivo* [26, 27], regulate both bone morphogenetic protein and type I collagen synthesis by osteoblastic cells [28] and modulate the osteoinduction of mesenchymal stem cells [29]. Additionally, we and others have shown that bioactive glasses sustain the expression of proangiogenic cytokines and indirectly induce angiogenesis *in vitro* [25, 30] and *in vivo* [10]. The *in vitro* mechanism of action of these bioactive ormoglasses has been

associated with the degradation of the CaP, leading to the release of physiologically relevant amounts of ions in the extracellular media [30-32]. *In vivo*, we have recently shown that, correlated with the Ca^{2+} release there was a significant expression of angiogenic factors, associated to a chemotactic effect on macrophages, what finally showed a significant increase of angiogenesis into the biomaterial [10].

As extracellular calcium has shown important roles both on proliferation, chemotaxis and differentiation of cells, and as elevated calcium levels have been described in the extracellular fluids of tissues suffering remodeling [33], namely bone, it has been proposed that increased calcium levels may act as paracrine regulators for various cellular functions.

Indeed, in the same line of we have recently shown [10], the injectable composite, containing 40% of ormoglasses cancined at 540ºC, shows a significant improvement in terms of angiogenesis. We assume that due to its faster Ca^{2+} release kinetics, in relation to the ormoglasses sintered at 570 ºC, it enables the release of Ca^{2+} in a range suitable for both improved osteogenesis and angiogenesis.

Altogether, one can assume that local elevated calcium levels may induce the recruitment of cells able to favor both a pro angiogenic milieu and to sustain bone formation. This approach allows in a simple and cost effective manner to address both the promotion of bone repair and to sustain angiogenesis.

5. Conclusions

We have developed an injectable composite, containing a CaP glass-ceramic dispersed within a HPMC matrix, with the capacity to release calcium in a controlled way. We show that by tuning the release of calcium, *in vivo*, we could improve both bone formation and also increase

angiogenesis. This methodology allows integrating two fundamental processes for bone tissue regeneration while using a simple, cost effective and safe approach.

6. References

[1] Brown KL, Cruess RL. Bone and cartilage transplantation in orthopaedic surgery. A review. J Bone Joint Surg Am 1982;64:270-9.
[2] Damien CJ, Parsons JR. Bone graft and bone graft substitutes: a review of current technology and applications. J Appl Biomater 1991;2:187-208.
[3] Ebraheim NA, Elgafy H, Xu R. Bone-graft harvesting from iliac and fibular donor sites: techniques and complications. J Am Acad Orthop Surg 2001;9:210-8.
[4] St John TA, Vaccaro AR, Sah AP, Schaefer M, Berta SC, Albert T, Hilibrand A. Physical and monetary costs associated with autogenous bone graft harvesting. Am J Orthop (Belle Mead NJ) 2003;32:18-23.
[5] Delloye C, Cornu O, Druez V, Barbier O. Bone allografts: What they can offer and what they cannot. J Bone Joint Surg Br 2007;89:574-9.
[6] Amini AR, Laurencin CT, Nukavarapu SP. Bone tissue engineering: recent advances and challenges. Crit Rev Biomed Eng 2012;40:363-408.
[7] Nguyen LH, Annabi N, Nikkhah M, Bae H, Binan L, Park S, Kang Y, Yang Y, Khademhosseini A. Vascularized bone tissue engineering: approaches for potential improvement. Tissue Eng Part B Rev 2012;18:363-82.
[8] Carragee EJ, Hurwitz EL, Weiner BK. A critical review of recombinant human bone morphogenetic protein-2 trials in spinal surgery: emerging safety concerns and lessons learned. Spine J 2011;11:471-91.
[9] Laschke MW, Harder Y, Amon M, Martin I, Farhadi J, Ring A, Torio-Padron N, Schramm R, Rucker M, Junker D, Haufel JM, Carvalho C, Heberer M, Germann G, Vollmar B, Menger MD. Angiogenesis in tissue engineering: breathing life into constructed tissue substitutes. Tissue Eng 2006;12:2093-104.
[10] Oliveira H, Catros S, Boiziau C, Siadous R, Marti-Munoz J, Bareille R, Rey S, Castano O, Planell J, Amedee J, Engel E. The proangiogenic potential of a novel calcium releasing biomaterial: Impact on cell recruitment. Acta Biomater 2016;29:435-45.
[11] Aguirre A, Gonzalez A, Planell JA, Engel E. Extracellular calcium modulates in vitro bone marrow-derived Flk-1+ CD34+ progenitor cell chemotaxis and differentiation through a calcium-sensing receptor. Biochem Biophys Res Commun 2010;393:156-61.
[12] Sanzana ES, Navarro M, Macule F, Suso S, Planell JA, Ginebra MP. Of the in vivo behavior of calcium phosphate cements and glasses as bone substitutes. Acta Biomater 2008;4:1924-33.
[13] Thebaud NB, Bareille R, Remy M, Bourget C, Daculsi R, Bordenave L. Human progenitor-derived endothelial cells vs. venous endothelial cells for vascular tissue engineering: an in vitro study. J Tissue Eng Regen Med 2010;4:473-84.
[14] Repetto G, del Peso A, Zurita JL. Neutral red uptake assay for the estimation of cell viability/cytotoxicity. Nat Protoc 2008;3:1125-31.
[15] Frohlich M, Grayson WL, Wan LQ, Marolt D, Drobnic M, Vunjak-Novakovic G. Tissue engineered bone grafts: biological requirements, tissue culture and clinical relevance. Curr Stem Cell Res Ther 2008;3:254-64.
[16] Woodruff MA, Lange C, Reichert J, Berner A, Chen F, Fratzl P, Schantz J-T, Hutmacher DW. Bone tissue engineering: from bench to bedside. Materials Today 2012;15:430-5.
[17] Gauthier O, Boix D, Grimandi G, Aguado E, Bouler JM, Weiss P, Daculsi G. A new injectable calcium phosphate biomaterial for immediate bone filling of extraction sockets: a preliminary study in dogs. J Periodontol 1999;70:375-83.

[18] Weiss P, Gauthier O, Bouler JM, Grimandi G, Daculsi G. Injectable bone substitute using a hydrophilic polymer. Bone 1999;25:67S-70S.
[19] Weiss P, Layrolle P, Clergeau LP, Enckel B, Pilet P, Amouriq Y, Daculsi G, Giumelli B. The safety and efficacy of an injectable bone substitute in dental sockets demonstrated in a human clinical trial. Biomaterials 2007;28:3295-305.
[20] Pickup DM, Abou Neel EA, Moss RM, Wetherall KM, Guerry P, Smith ME, Knowles JC, Newport RJ. Ti K-edge XANES study of the local environment of titanium in bioresorbable TiO2-CaO-Na2O-P2O5 glasses. J Mater Sci Mater Med 2008;19:1681-5.
[21] Pickup DM, Guerry P, Moss RM, Knowles JC, Smith ME, Newport RJ. New sol-gel synthesis of a (CaO)0.3(Na2O)0.2(P2O5)0.5 bioresorbable glass and its structural characterisation. Journal of Materials Chemistry 2007;17:4777-84.
[22] Navarro M, del Valle S, Martinez S, Zeppetelli S, Ambrosio L, Planell JA, Ginebra MP. New macroporous calcium phosphate glass ceramic for guided bone regeneration. Biomaterials 2004;25:4233-41.
[23] Castano O, Sachot N, Xuriguera E, Engel E, Planell JA, Park JH, Jin GZ, Kim TH, Kim JH, Kim HW. Angiogenesis in bone regeneration: tailored calcium release in hybrid fibrous scaffolds. ACS Appl Mater Interfaces 2014;6:7512-22.
[24] Lee GH, Hwang JD, Choi JY, Park HJ, Cho JY, Kim KW, Chae HJ, Kim HR. An acidic pH environment increases cell death and pro-inflammatory cytokine release in osteoblasts: the involvement of BAX inhibitor-1. Int J Biochem Cell Biol 2011;43:1305-17.
[25] Aguirre A, Gonzalez A, Navarro M, Castano O, Planell JA, Engel E. Control of microenvironmental cues with a smart biomaterial composite promotes endothelial progenitor cell angiogenesis. Eur Cell Mater 2012;24:90-106; discussion
[26] Adams GB, Chabner KT, Alley IR, Olson DP, Szczepiorkowski ZM, Poznansky MC, Kos CH, Pollak MR, Brown EM, Scadden DT. Stem cell engraftment at the endosteal niche is specified by the calcium-sensing receptor. Nature 2006;439:599-603.
[27] Tommila M, Jokilammi A, Terho P, Wilson T, Penttinen R, Ekholm E. Hydroxyapatite coating of cellulose sponges attracts bone-marrow-derived stem cells in rat subcutaneous tissue. J R Soc Interface 2009;6:873-80.
[28] Nakade O, Takahashi K, Takuma T, Aoki T, Kaku T. Effect of extracellular calcium on the gene expression of bone morphogenetic protein-2 and -4 of normal human bone cells. J Bone Miner Metab 2001;19:13-9.
[29] Gonzalez-Vazquez A, Planell JA, Engel E. Extracellular calcium and CaSR drive osteoinduction in mesenchymal stromal cells. Acta Biomater 2014;10:2824-33.
[30] Day RM. Bioactive glass stimulates the secretion of angiogenic growth factors and angiogenesis in vitro. Tissue Eng 2005;11:768-77.
[31] Keshaw H, Forbes A, Day RM. Release of angiogenic growth factors from cells encapsulated in alginate beads with bioactive glass. Biomaterials 2005;26:4171-9.
[32] Leu A, Leach JK. Proangiogenic potential of a collagen/bioactive glass substrate. Pharm Res 2008;25:1222-9.
[33] Brown EM, MacLeod RJ. Extracellular calcium sensing and extracellular calcium signaling. Physiol Rev 2001;81:239-97.